Upcycling of PET plastics into diethyl terephthalate for applications as phase change materials in energy harvesting

Johnathan Joo Cheng Lee [a,1], Nur Nawwarah Ainul Hayat [b,1], Xiang Yun Debbie Soo [a], Sze Yu Tan [a], Yu Yu Koh Hnin [a], Suxi Wang [a], Fengxia Wei [a], Dai Kai [a,c], Fuke Wang [a], Ping Luo [a], Jianwei Xu [a,c,d], Xian Jun Loh [a,c,e,*], Qiang Zhu [a,c,f,*]

[a] Institute of Materials Research and Engineering, A*STAR (Agency for Science, Technology and Research), 2 Fusionopolis Way, Innovis, #08-03, Singapore 138634, Singapore
[b] Faculty of Science, Jalan Tungku Link, Gadong, Universiti Brunei Darussalam, BE1410, Brunei Darussalam
[c] Institute of Sustainability for Chemicals, Energy and Environment, A*STAR (Agency for Science, Technology and Research), 1 Pesek Road, Jurong Island, Singapore 627833, Singapore
[d] Department of Chemistry, National University of Singapore, 3 Science Drive 3, Singapore 117543, Singapore
[e] Department of Material Science and Engineering, National University of Singapore, 9 Engineering Drive 1, #03-09 EA, Singapore 117575, Singapore
[f] School of Chemistry, Chemical Engineering and Biotechnology, Nanyang Technological University, 21 Nanyang Link, Singapore 637371, Singapore

ARTICLE INFO

Keywords:
Phase change materials
Thermal energy storage
Upcycling
Sustainability
Building
Green chemistry

ABSTRACT

Polyethylene terephthalate (PET) is an indispensable material in our everyday lives and upcycling of its waste has become a major area of research. Herein, the upcycling of PET waste into phase change materials (PCM) for thermal energy storage applications is presented. Hydrolysed and esterified PET waste affords diethyl terephthalate (DET), which when blended with UV-curing acrylic matrix, trimethylolpropane ethoxy triacrylate (TMPEOTA), forms a composite PCM. Chemical characterisation such as IR and NMR were conducted to confirm the presence of functional groups in the composites. The thermal properties of the composites, such as melting point and thermal degradation were obtained and DET exhibited a relatively high melting enthalpy of 94.1 J/g at about 39.9 °C. The form stability and thermal performance was studied for composites made of different DET loading weight percentages from 50 to 90 %. A loading rate of 80 % (D80) was found to provide best latent heat capacity while maintaining its form stability and minimizing leakage. Finally, to assess the performance of D80 as a thermal storage material, a thermal response test was performed and D80 was able to prevent significant rise in temperature for about 60s during its phase transition as opposed to TMPEOTA control.

1. Introduction

According to the Organisation for Economic Co-operation and Development (OECD), approximately 353 million tonnes of plastic waste were generated globally from 2000 to 2019, with only 9 % and 19 % recycled and incinerated, respectively [1,2]. More than 50 % of the plastic waste incinerated ended ultimately in the rivers and oceans, contributing to CO_2 emissions and environmental pollution [3,4]. A proposed solution to this problem is to valorise the plastic waste to give it a "second life" [5–7]. Upcycling is the process of converting used or waste materials in their end-of-life stage into something of greater value via a creative reuse method [8,9]. Upcycling is a good strategy to regenerate the value of plastics and is widely regarded as one of the potential solutions to plastic waste in the future [10,11]. In today's society, one of the most heavily utilized plastics is PET (polyethylene terephthalate). The popularity of PET stems from its high strength-to-weight ratio [12–14], and antifouling and antimicrobial properties. PET is generally inert, thus, widely accepted by health authorities as a safe plastic material for most food and beverages packaging [15–17]. However, what makes it so attractive also prevents wearing and breaking down of the PET waste naturally [18–21]. Hence, upcycling of PET plastics plays an important role in tackling environmental pollution

* Corresponding authors at: Institute of Materials Research and Engineering, A*STAR (Agency for Science, Technology and Research), 2 Fusionopolis Way, Innovis, #08-03, Singapore 138634, Singapore.
E-mail addresses: lohxj@imre.a-star.edu.sg (X.J. Loh), zhuq@imre.a-star.edu.sg (Q. Zhu).
[1] Both authors contribute equally to this work.

https://doi.org/10.1016/j.est.2023.109084

contributed by plastic waste.

The valorisation of PET into useful functional materials, particularly into Phase Change Materials (PCM), has attracted considerable attention. PCM are valued for their efficiency in thermal properties and energy storage due to their high latent heat and recyclability [22–25]. However, issues such as leakage of PCM in composite PCM material during phase change have posed a problem in practical applications [26,27]. Serious leakage during phase transition can be prevented through the use of form stable PCM (FSPCM) composites [28]. FSPCM composites absorb PCM into an additive material, such as porous inorganic materials [29,30] through capillary forces and interfacial tension within the pores via vacuum impregnation [31]. Above the phase transition temperature, FSPCM composites prevent leakage of PCM and retain their shape [32]. This is due to the composite materials possessing advantageous traits of the constituents in comparison with individual components in various applications [33–36]. To date, there have been several strategies to fabricate FSPCM such as through processes such as mixing and blending composites into the PCM, sintering using heat [31] and pressure [37], stabilisation by forming crosslinking networks to hold the PCM in place in curable materials [38] or immersion to form encapsulations [39] or impregnated composites [40–42]. Towards understanding the mechanism of the phase transitions behaviours, various research has been conducted [43–45]. FSPCM composites also involve the combination of organic polymer matrix with PCM via melt blending method or engaging an extruder [25,46]. In context of PET breakdown products, for instance, Ram et al. reported the use of microencapsulated dimethyl terephthalate composite PCM as a form stable PCM with a relatively high latent heat of 118 J/g [47]. In addition, PET plastics have been shown to reduce cleanly to terephthalic acid and ethylene glycol or bis-hydroxy(2-ethyl) terephthalate, among others [48,49].

Recently, our group made use of a curing matrix to form a FSPCM [24]. Polymers commonly used as curable PCM composites include epoxy [50], acrylic [51], polyurethane [52] and polyethylene [53]. In particular, the use of UV radiation efficiently cures coatings such as paints within seconds [54]. Acrylates are excellent candidates as coating additives for surfaces such as exteriors of buildings [23,55]. These coatings and paints need almost no solvents and, in most cases, less energy is consumed [56]. We reported the use of a crosslinking UV curable acrylate TMPEOTA as an efficient additive for the fabrication of form stable composite PCMs [24]. Other reports also showcased the use of UV curable matric for effective form-stability characteristics such as polyurethane-acrylate coating developed by Jae et al. for polyol type adhesive properties [38]. In a similar use of polyurethane acrylate matrix, Li et al. made use of myristic acid with the UV curable matrix as low temperature thermal energy storage material [57]. UV-cured surfaces are long-lasting and resistant to abrasion and scratching [58]. Radiation-cure technology and more specifically the UV-cure technology is among the rapidly growing and very promising coating technologies due to their low environmental impact, low energy consumption, high efficiency, and contribution towards safe and healthy working environment, combined with acceptable performance of their coatings [59,60]. In this work, we report the upcycling of PET plastic waste in gram scale by hassle free purification procedures and thereafter through simple cold crystallisation. We also report the use of DET as a PCM for potential application as a coating or paint material on buildings for heat storage management as it exhibits high latent heat at 39.8 °C which is a temperature expect for building components to reach when heated by the solar radiation. We examine the form stability and leakage of an FSPCM made of DET incorporated into composites with UV curing TMPEOTA matrix when the FSPCM is subjected to temperatures higher than the melting temperature of PCM. Furthermore, the thermophysical properties of the FSPCM are studied and the suitability of FSPCM for thermal storage applications is studied by conducting a heat absorption test. We find that.

2. Materials and methods

2.1. ATR-FTIR analysis of DET, TMPEOPTA and the composites

Functional group identification of prepared samples was studied using attenuated total reflection Fourier transform infrared spectroscopy (ATR-FTIR) on an infrared spectrometer (Spectrum 2000, PerkinElmer, USA). Each sample was examined using 16 scans with a resolution of 1 cm^{-1} between 4000 and 600 cm^{-1}.

2.2. Thermal properties analysis

The thermal stability of DET, TMPETOA and the composites were examined using the thermogravimetric analyser TGA Q500 by TA Instruments. The samples were heated up to 550 °C at a rate of 20 °C/min under dynamic nitrogen atmosphere (flow rate = 50 ml/min). Differential scanning calorimetry (DSC) thermal analysis was performed using a differential scanning calorimeter (Q100, TA Instruments, USA) equipped with an auto cool accessory and calibrated using indium. The following protocol was used for the composite samples: heating from room temperature to 70 °C at 20 °C/min, holding at 70 °C for 2 min, cooling from 70 °C to —20 °C at 20 °C/min, hold at —20 °C for 2 min, and finally reheating from —20 to 70 °C at 20 °C/min.

2.3. Scanning electron microscopy

The morphologies of the samples were observed using a field electron scanning electron microscope (FESEM, SU8220, Hitachi, Ltd., Tokyo, Japan) and for a standardized and fair comparison, the images were all taken at magnification ×500. The samples were examined under room temperature and coated with 3–5 Å of Pt to remove charging in the sample.

2.4. Upcycling route of DET from PET plastics

The synthesis route is as shown in Fig. 1. PET plastic (shredded plastic containers/bottles purchased from commercial sources) was washed, dried and vacuum dried overnight prior to use in the synthesis for removal of impurities. Weighed amount of shredded PET plastics (5 g) was placed in a round beaker flask charged with a magnetic stir bar. Concentrated HCl was then added dropwise and the mixture was heated and stirred overnight at 500 rpm. Thereafter, 500 ml of EtOH was added in situ and heated up to reflux overnight. Thereafter, the solution became pale yellow, the reaction was quenched by pouring the reaction mixture into cold water. The DET precipitates were obtained via vacuum filtration and rinsed with cold water. No further purification was required and DET was used directly for fabrication of the composite.

2.5. Preparation of physically mixed samples

The physically mixed samples were prepared by mixing the as-prepared DET powder and liquid acrylate monomer of TMPEOTA in 2 ml vial to obtain a composite mixture as seen in Fig. 1. The two components were weighed based on their specific wt% and made to a weight of 0.2 g. Five composite samples were prepared, namely, D50, D60, D70, D80 and D90, where DX0 indicates the percentage of DET present. Thereafter, the vials were exposed to 395 nm UV irradiation for 2 s running over a conveyer belt three times and allowed to cool to room temperature thereafter.

The mechanism in which TMPEOTA encompasses DET, illustrated in Fig. 2, is based on a photo-induced polymerization reaction of the three terminal vinyl groups on the monomer of TMPEOTA with the help of a photo initiator. The suggested mechanism was illustrated according to concepts from Zhu et al. [61,62]. Upon UV irradiation, the photo initiator (in this case TPO) undergoes homolytic bond cleavage and one of the radical species like the phosphate radical will scavenge on the

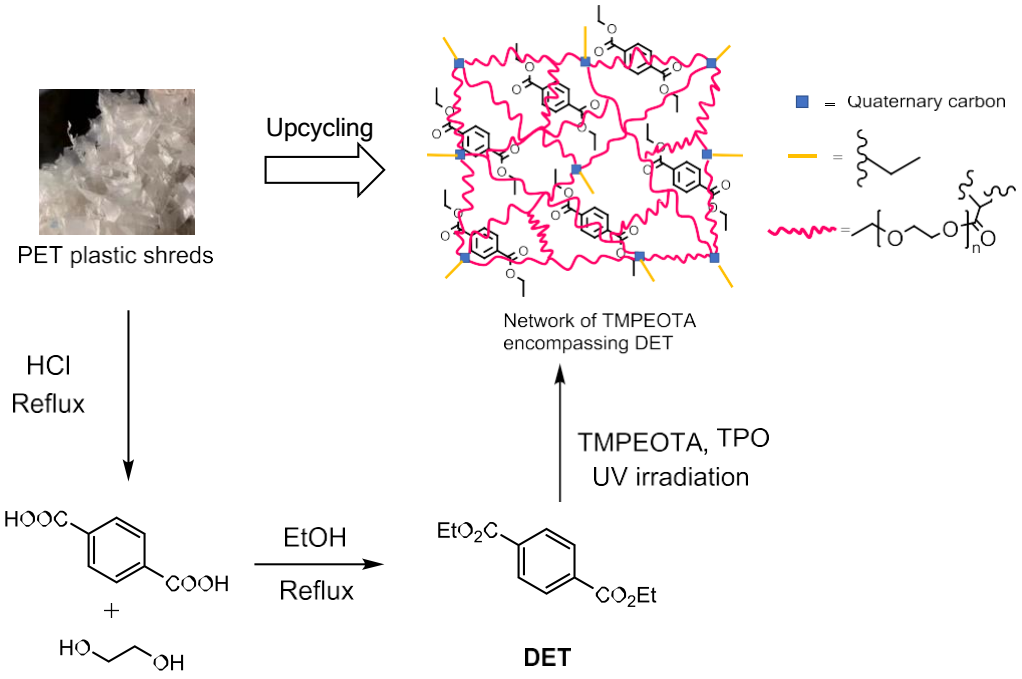

Fig. 1. Upcycling route of PET to DET composites.

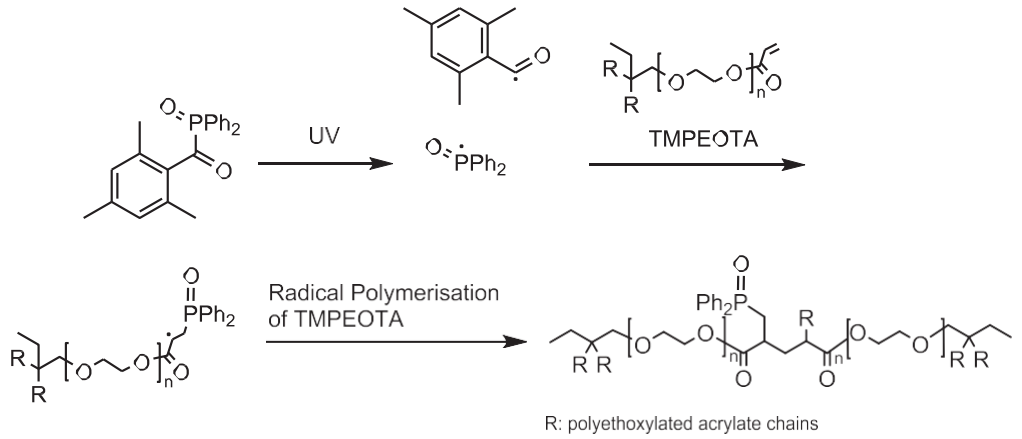

Fig. 2. Upcycling route of PET to DET composites.

electron rich pi electrons of vinyl group. This affords a radical species on the TMPEOTA chain which is then ready to propagate by scavenging for more TMPEOTA cascading into a radical polymerization. The polymerization affords a highly branched network of polyethoxylated acrylates which traps and hold the DET small molecules in the matrix, preventing DET from leaking out of the matrix when heated above its melting temperature. A detailed mechanism of the polymerization was also illustrated for clearer interpretation of the mechanism.

2.6. Form stability test

DET, TMPEOTA and the composite samples were prepared in a 2 ml vial based on the weight percentage and were heated to their melting temperatures. The samples were cured under exposure to UV irradiation, the 2 ml vials were then inverted, and placed in the oven at 2 different temperatures (40 and 65 °C). At regular time intervals, the vials were taken out for image capture and form-stability assessment through visual inspection of leakage, thereafter they were placed back into the oven for a total duration of 1 days.

2.7. Leakage test

A piece of the composite samples (D50–D90) were prepared and placed on a piece of filter paper for leakage test as described by Sari and Hekimog˘lua et al. [63]. The initial weights of the samples were recorded before being exposed to melting temperatures (similar to Section 2.6) in the oven overnight (40 °C and 65 °C). The samples were then taken out and the final weight of the sample was weighed and recorded immediately. Visual inspection and photographs were also taken to recorded traces of any leakage stains left on the filter paper as 'damp' spots.

3. Results and discussion

3.1. Upcycling process of PET to DET

DET was obtained in quantitative yield from an in-situ and straight forward upcycling synthesis using PET plastics waste as described in Section 2.4. The procedure is clean and green as it does not involve heavy metal catalyst or any harmful solvents. The synthetic route begins

with shredded PET plastics from used bottles. The shreds are stirred with dropwise addition of concentrated HCl under reflux condition to obtain terephthalic acid and ethylene glycol upon acid hydrolysis of the PET polymer. After complete hydrolysis of the PET shreds to terephthalic acid and ethylene glycol, excess amount of EtOH is added into the reaction mixture and refluxed overnight to allow esterification terephthalic acid to form DET. DET precipitated in cold water, wash and filtered under vacuum filtration. No further purification is required. The ^{1}H NMR of the product is shown in Fig. 3. The singlet at 8.08 ppm is representative of the proton on the phenyl group while the quartet peak at 4.35 ppm corresponds to the protons of the methine group of the ethyl ester and the triplet peak at 1.41 ppm corresponds to protons of the methyl peak of DET.

3.2. SEM imaging

Scanning Electron Microscopy was conducted to examine the surface morphology of the composite PCM samples. It can be observed that the physically mixed samples displayed star-shaped crystalline structures evident in the smooth regions that are more apparent as the content of DET increases as seen in Fig. 4a–e. The pure sample of DET is seen in Fig. 3f depicts a homogeneous smooth surface. In composite samples seen in Fig. 3a–e, star-shaped structures can be attributed to the crystallisation of DET during the curing of the composite sample as low melting point components, like DET, tend to crystallise easily upon cooling. The crystallisation of DET onto a cooled surface under UV irradiation process, suggests a phase separation between the two components. This is due to incompatible solubility of DET in TMPEOTA as their unfavourable enthalpic interaction and low entropy of mixing of the long chain acrylates [64]. The phase separation prevents a homogeneous solution from forming and causes domains of the two components to be observed.

3.3. FT-IR analysis

FT-IR spectra of the composite samples, TMPEOTA and DET are shown in Fig. 5. The presence of a distinct and intense peak around 1711 cm^{-1}, is characteristic of the typical stretching frequency of carbonyl C^{-}O bond in ester linkages of the two different ester groups in DET (1720 cm^{-1}) and TMPEOTA (1709 cm^{-1}) are observed in the composite samples and their peak intensity corresponds to the ratio of each component. Additionally, a peak at 1260 cm^{-1} confirmed the presence of C–O bonds which was also observed in both DET and TMPEOTA sample. These two peaks justified the presence of ester linkages in DET and TMPEOTA of both components. The broad shoulder peak in all samples around 2940 cm^{-1} can be ascribed to the aromatic and aliphatic C–H stretching in both TMPEOTA and DET. The broad shouldering C–H stretching peak of DET at 2869 cm^{-1} gradually intensifies as the DET loading increases from D50 to D90 while the characteristic C–H stretching peak of TMPEOTA of 2958 cm^{-1} gradually diminishes as the loading of the acrylate decreases from D50 to D90.

3.4. TGA analysis

TGA analysis was conducted to study the thermal stability of the samples as shown in Fig. 6. The pristine compounds of DET and TMPEOTA both exhibits a one-step degradation at 250 °C and a two-step degradation at about 375 and 450 °C respectively. The two-step degradation of TMPEOTA was mainly due to multiple mixing of the monomer in the system [57,65]. In the case of the composite samples, their degradation characteristics are combinations of both the DET and TMPEOTA as their degradation processes coincides with that of DET at about 200 °C (first degradation) and TMPEOTA about 375 and 410 °C (second and third degradation). These results also suggest the samples thermally stable during their operating temperatures at around 40 °C and high purity of the samples as it only exhibits the degradation that is attributed to the two components in the samples. In additional, the amount of initial degradation corresponds to the loading of DET present in the sample. All samples are completely degraded at about 700 °C as the compounds are mostly oxidized to CO_2 and H_2O when weight percentage approaches near 0 %. This suggests a relatively clean degradation process of releasing mainly carbonaceous gases such as CO, CO_2 and CH_4 without the formation of unwanted side products upon high heat.

3.5. DSC analysis

To examine the melting temperatures of the samples, DSC analysis was conducted and the thermograms are illustrated in Fig. 7. Their thermal parameters are also tabulated and summarised in Table 1 for easier comparison. It was observed from the thermograms that all

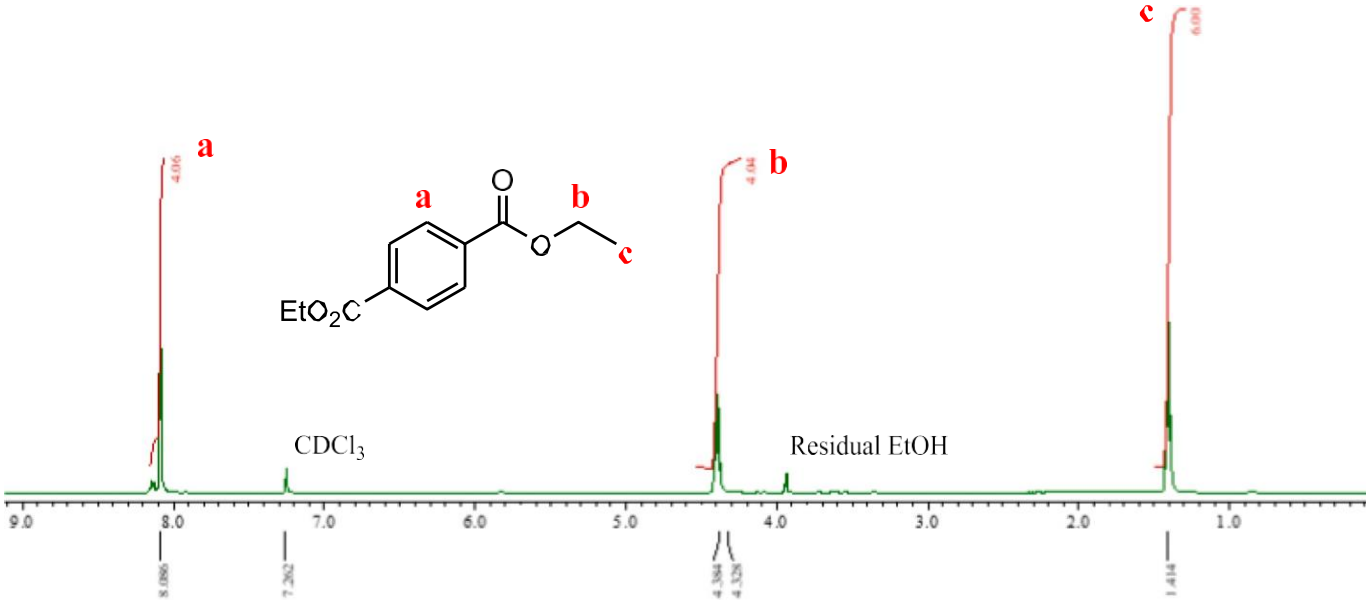

Fig. 3. ^{1}H NMR of DET after esterification in EtOH.

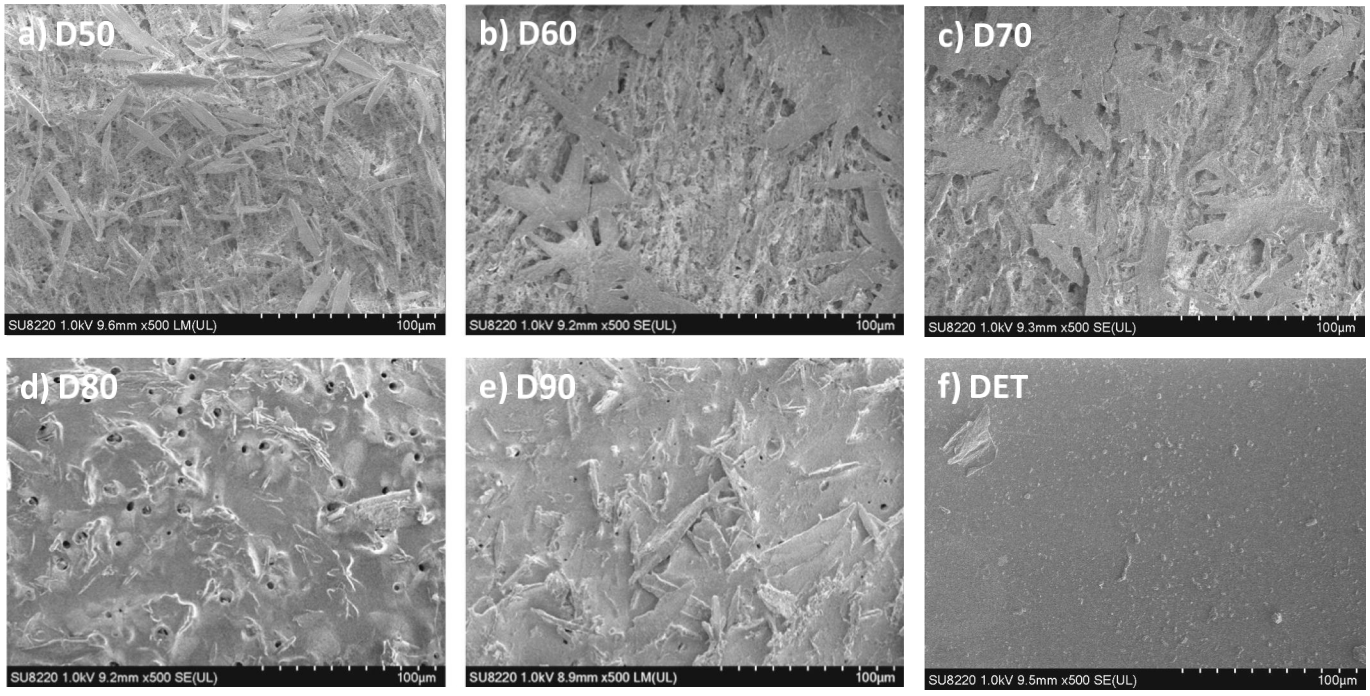

Fig. 4. SEM images of the surface morphology of a) D50 b) D60 c) D70 d) D80 e) D90 f) DET.

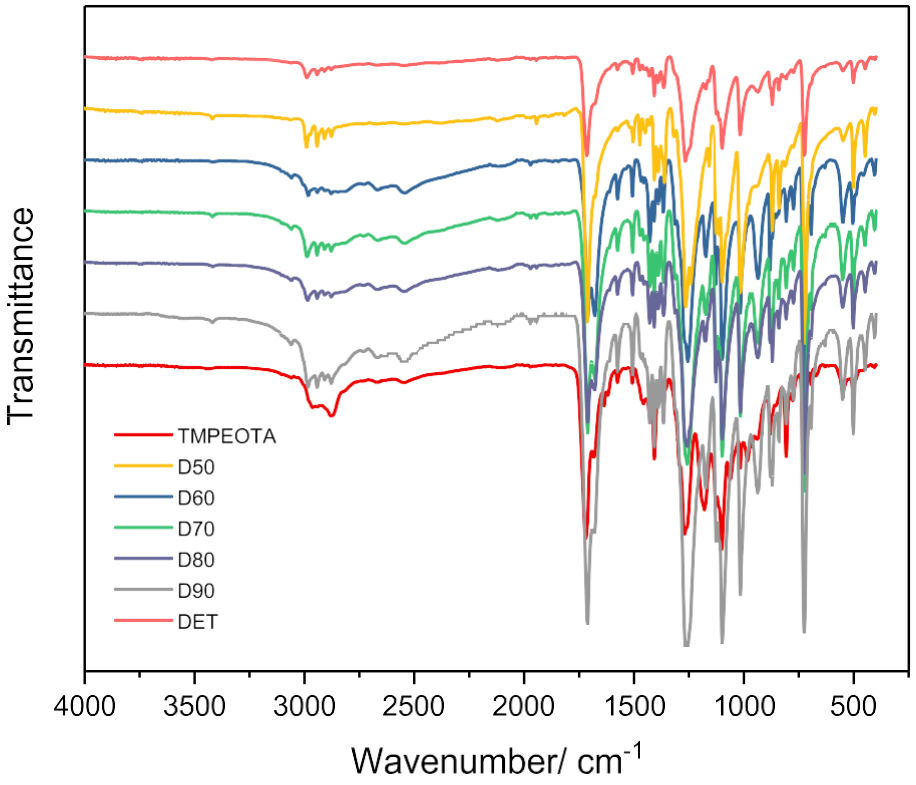

Fig. 5. FT-IR analysis of the composite PCMs and the pristine components.

samples have a single melting point of around 40 °C, which is attributed to the DET that is present in the sample. Samples with higher wt% loading of DET have a higher melting enthalpy due to lower hinderance and impurities to the crystallinity of DET by TMPEOTA. Ideally, the addition of TMPEOTA should not have any influence on the melting enthalpy and that the enthalpy of the sample should be proportional to the content of DET present. Thus, the theoretical melting enthalpy can be determined from the melting enthalpy of pure DET and the ratio of DET present in the sample. However, all the experimental melting enthalpies exhibited lower than theoretical values.

Based on the concept of crystallinity, it is known that small molecules, such as DET, form crystalline domains when their symmetrical three-dimensional arrangements are thermodynamically favoured, resulting in crystalline solids. The 3-D ordered organisation of DET is

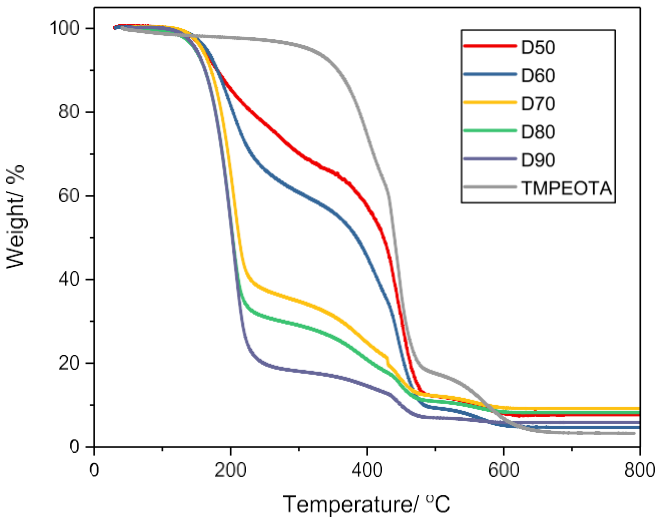

Fig. 6. TGA analysis of the composite PCMs and the pristine components.

affected (and hence hampered) by the incorporation of TMPEOTA as a supporting matrix, which disrupts its crystallinity. By this in turn, the discrepancy of the theoretical and experimental melting enthalpy during the phase change increase as the content of TMPEOTA increases. The larger discrepancy in D50 (difference of 25.4 Jg^{-1}) as compared to D90 (difference of about 1 Jg^{-1}) is due to the larger degree of disruption in crystallinity of DET. Based on this justification, the macropolymeric dense network of highly branched TMPEOTA causes lattice defects in the crystal lattice of DET since DET crystalises readily upon cooling, resulting in a lower degree of crystallinity and affecting the melting enthalpy of DET.

3.6. *Thermal stability test*

To access the thermal reliability of D80, a thermal stability study using DSC cycling and phase change behaviour of D80 was conducted between —20 °C to 70 °C for 100 cycles. The analysis was recorded via repeated heating and cooling and illustrated in Fig. 8. Based on the thermogram, we can justify that the excellent thermal reliability and stability of D80 as the melting temperature from the thermogram does not show much deviation from the original melting point of D80. Based on the DSC thermal cycling, the 2nd, 25th, 50th, 75th and 100th cycles are overlapped, the results showed that there is a 4.8 % decrease in melting enthalpy of the D80 sample between the 2nd and 100th cycle of the D80 sample. The negligible difference in melting enthalpy and melting point supported the thermal stability of D80.

3.7. *Form stability study*

A form stability test as described in Section 2.6 was conducted to assess and determine the sample with the highest latent heat via amount of PCM loading in response to different temperatures. Mainly, the melting temperature of DET at 40 °C and a higher temperature beyond its melting pointing point at 60 °C. Fig. 9a shows the initial state of the sample as it is cured and inverted at room temperature before heating in the oven. Upon exposure to the melting temperature of 40 °C of DET for 24 h, the samples are photographed as depicted in Fig. 9b. It is observed that the pristine DET had drastic leakage. At this point, D90 also exhibited signs of leakage and this was expected as the amount of

Table 1
Melting enthalpy if the composite samples and DET.

Sample	Theoretical melting enthalpy/ Jg^{-1}	Experimental melting enthalpy/ Jg^{-1}
D50	47.0	21.6
D60	56.4	30.5
D70	65.8	51.3
D80	75.2	55.9
D90	84.69	83.6
DET	94.1	94.1

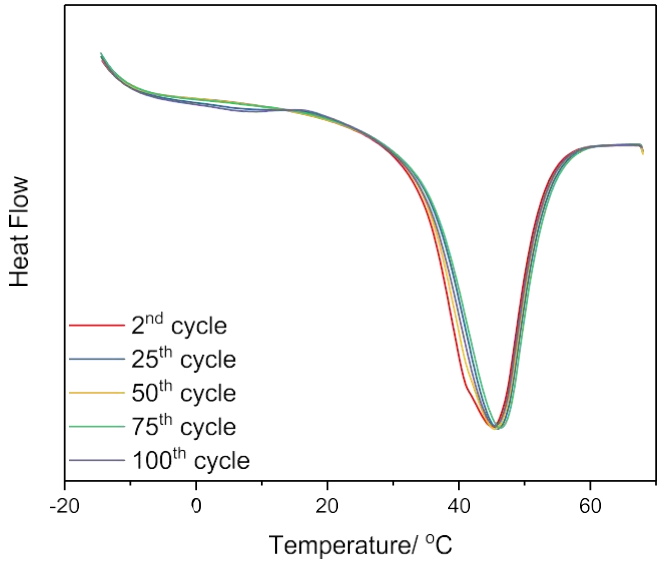

Fig. 8. DSC cycling stability analysis showing curve of D80 at 2nd, 25th, 50th, 75th and 100th cycle.

Sample	Theoretical Melting Enthalpy / Jg^{-1}	Experimental Melting Enthalpy / Jg^{-1}
D50	47.0	21.6
D60	56.4	30.5
D70	65.8	51.3
D80	75.2	55.9
D90	84.69	83.6
DET	94.1	94.1

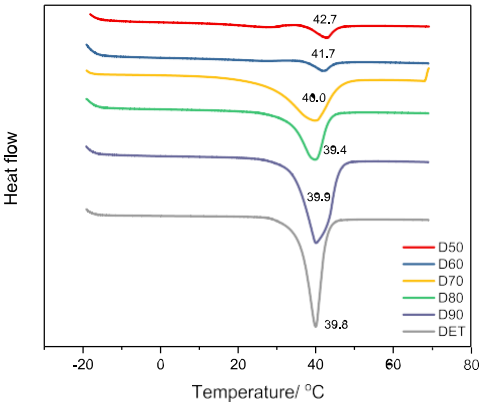

Fig. 7. DSC analysis of the composite samples and DET.

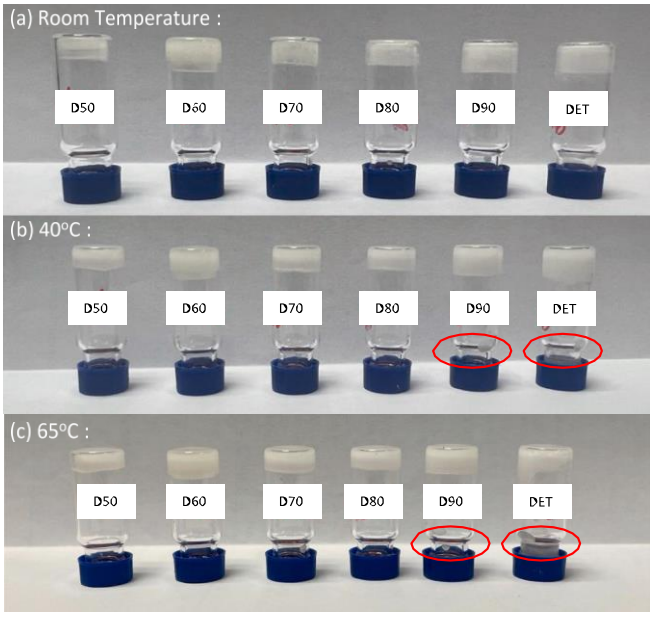

Fig. 9. Form stability test of the composite samples and DET at a) room temperature b) melting temperature of DET ~40 °C and c) above melting temperature at 65 °C. (Red circles marking leakage in the samples). (For interpretation of the references to color in this figure legend, the reader is referred to the web version of this article.)

TMPEOTA was insufficient to prevent the melted DET from leaking. In the case of pure DET, it does not have an external binder to keep its form in place upon melting. Meanwhile, the content of TMPEOTA in D90 was insufficient to bind the amount of DET in place resulting in sample leakage. Conversely, the samples of D50 to D80 showed no signs of any sample leakage indicating that the amount of TMPEOTA was sufficient to hold the sample intact preventing leakages. At temperature beyond their melting temperatures, the samples are pushed beyond its performance limit to access its durability. Surprisingly at 65 °C, D50–D80 continued to remain intact and showed excellent form stability with no signs of leakages while D90 and pure DET samples exhibited serious leakages observed in Fig. 9c. This suggest the efficiency of the 3-D interlocking network of TMPEOTA in trapping DET in is matrix to prevent sample leakages even beyond its melting temperature as illustrated in Fig. 9d.

3.8. Leakage test

To further support the form stability test above, a more quantitative way to assess its form stability is to conduct a leakage test. As described in Section 2.7, the samples were placed on a filter paper at a temperature above 40 °C then to 60 °C, which is the temperature at which are beyond the melting temperatures of DET as depicted in the photographs in Fig. 10. Upon exposure to its melting temperature range at 40 °C, D50 to D80 kept its form while leakage is already observed in D90. The leakage stain was visible after the samples were taken out of the filter paper. D50 to D80 starts to show signs of leakage at temperatures greater than its melting point of about 65 °C of about 4.1 %. The test results were calculated and summarised in Table 2. Noteworthy is the significantly lower leakage observed from D80 (9.2 % as compared to 18 % in D90) onwards with D50 showing the least leakage. The leakage was determined by weighing the sample before and after the test. As the TMPEOTA matrix are higher in loading, the highly branched networks of TMPEOTA are able to trap and hold the individual DET in place preventing the lowest leakage in D50. We can also suggest that the balance between form stability and thermal properties of the composites was optimum at around D80 as any additional content of DET added will result in drastic increase in leakage.

3.9. Thermal performance test

Thermal performance of D80 was investigated and compared against pure TMPEOTA as a reference standard. Based on the form stability test, D80 the highest latent heat with the highest PCM loading composite while maintaining form stability at temperatures beyond its melting temperature. A plot of temperature changes against time is shown in

Table 2
The initial and final weight of the composite sample during the leakage test and the percentage of leakage calculated from the test.

Sample	Initial weight (g)	Final weight after leakage test (g)	Leakage (%)
D50	0.326	0.312	4.1
D60	0.186	0.173	6.8
D70	0.140	0.127	9.0
D80	0.125	0.115	9.2
D90	0.171	0.140	18.0

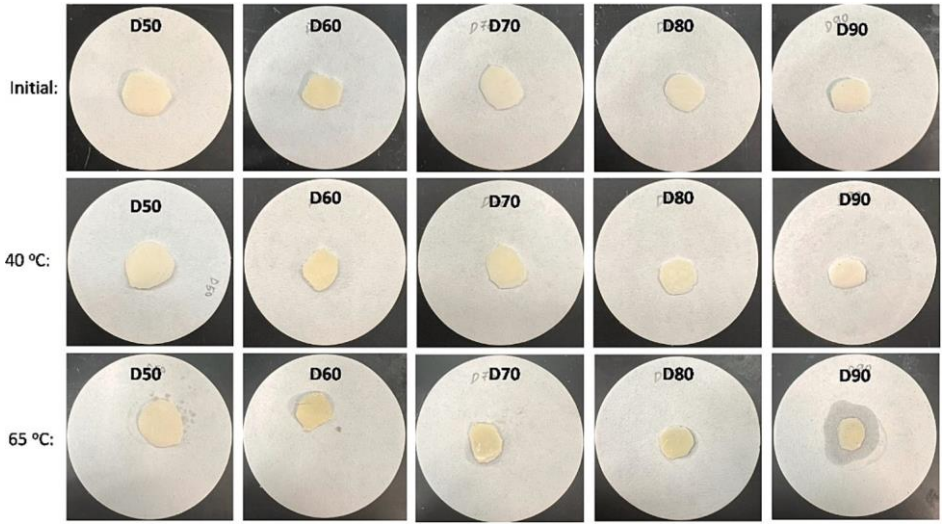

Fig. 10. Photographs taken during the process of the leakage test at 40 °C, after higher temperature of 6 °C were taken and the leakage stain are observed as 'damp spots' on the filter paper.

Fig. 11a depicted the thermal performance of D80 and TMPEOTA over time in response to changes in temperature. IR images of the samples were also photographed at different time intervals to show the heat absorption and storage performance of the samples.

The samples were set up by placing both D80 and TMPEOTA, as a standard, on a heating mantle as the temperature was gradually raised to around 70 °C (Fig. 11b). When the temperature gradually rises, TMPEOTA temperature rises rather quickly. However, in the case of D80, we observed a much slower increase in temperature and the rate of heating even slows down to almost a plateau at about 50 s. This was believed to be attributed to the phase change od DET in the sample thus resisting the temperature change. This phenomenon continued to persist for about 60s, thereafter, the temperature rose quickly, similar to rates of the sample of TMPEOTA. Visual evidence of IR also shows slower heating rates of D80 as compared to TMPEOTA (Fig. 11c) This suggests that all the DET have been supplied with sufficient energy to undergo phase transition and are not able to store any more heat. Both samples eventually attained a maximum temperature of about 70 °C as observed in the IR images (Fig. 11d). Thereafter, upon switching off the heating mantle, gradual cooling process of the sample begins. It is observed that TMPEOTA cools at a faster rate as compared to D80.

This phenomenon is expected as D80 is able to store heat better than TMPEOTA as evident in the IR image in Fig. 11e. D80 continue to cool at a slower rate than TMPEOTA maintaining a high temperature over a period, IR images of the samples also continue to show that D80 displays a warmer tone as compared to TMPEOTA. At about 300 s, the temperature differences of the two samples becomes less obvious as seen in Fig. 11f as they have almost cooled to the room temperature. At 400 s, both samples have completely cooled and solidified at room temperature, as depicted in Fig. 11g. Through this heat absorption performance test, we can conclude that D80 has the potential to be applied as a thermal regulating material for operational temperatures near 36–40 °C which is within D80's as it falls in its phase change temperature. Some possible applications to infrastructures may be in water tanks for thermal heating purposes or concrete wall panels for thermal heating, or thermoelectric since the operating temperature falls within the phase change temperature of D80 [66,67].

4. Conclusion

To conclude, the thermal storage capabilities of PCM was showcased in upcycled products of PET waste plastics, in this case DET was examined for its PCM properties and its ability for store latent heat. Several samples of DET of different loading weight was prepared with TMPEOTA matrix to prevent leakage of the PCM during its performance. D80 was determined to be the best performing candidate with the highest amount of latent heat but at the same time retaining its form stability when heated above its melting temperature. We successfully analysed and characterised the samples via TGA and DSC to study their thermal properties and FTIR and SEM to study the chemical and physical evidence of the samples, respectively. Cyclic thermal stability test also showed good thermal reliability of D80 sample as the latent heat deviated minutely from the original value. We also showcased the potential of D80 as a thermal storage material by studying its heat absorption and response to temperature changes over time as compared to the control TMPEOTA. We observed that as the temperature is raised to above the melting temperature of D80 the rate of heating was much slower as compared to the control due to its phase transition. This suggest potential application of D80 as coating materials for surfaces which may be used for thermal storage or heat comfort. Lastly, we hope that this study helps to bring more insights in the possibilities of upcycling and its huge potential in sustainability and reusable energy.

CrediT authorship contribution statement

Johnathan Joo Cheng Lee: Conceptualization, Writing – Original Draft
Nur Nawwarah Ainul Hayat: Writing – Original Draft
Xiang Yun Debbie Soo: Conceptualization and Ideas of Original Draft
Sze Yu Tan: Contribution to instrumental Analysis
Yu Yu Koh Hnin: Contribution to instrumental Analysis
Fengxia Wei: Conceptualization and Ideas of Original Draft
Dan Kai: Conceptualization, Supervision
Fuke Wang: Visualization, Review & Editing
Ping Luo: Contribution to instrumental Analysis
Jianwei Xu: Writing – Review & Editing, Supervision
Xian Jun Loh: Visualization, Supervision

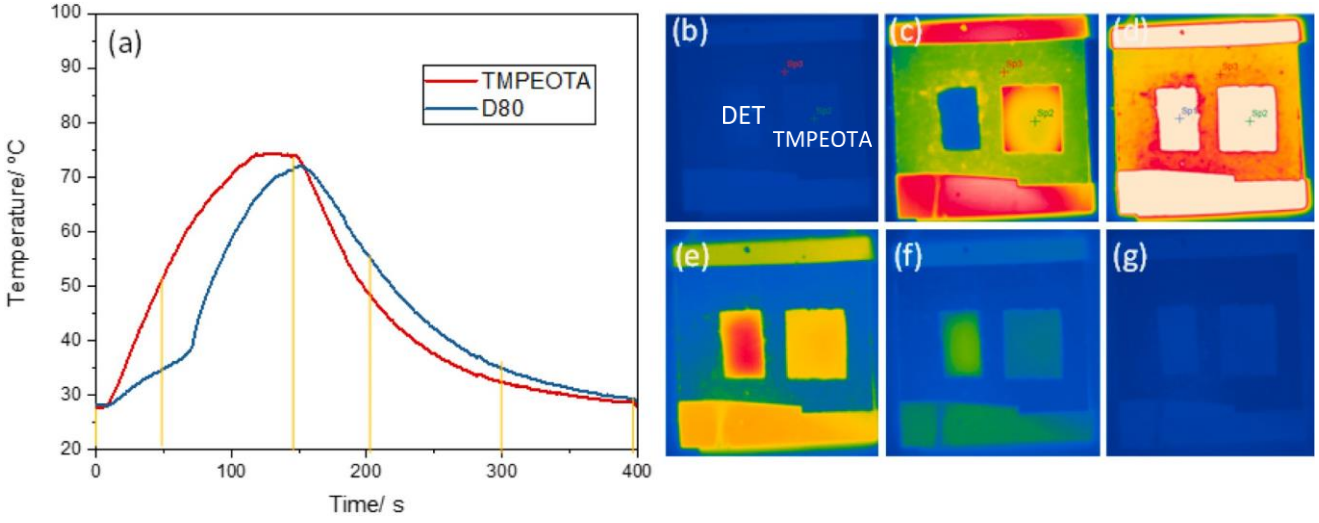

Fig. 11. a) A plot of temperature against time of D80 in comparison with TMPEOTA when exposed to heating and cooling. Time stamps of significant changes in the samples were imaged using IR camera b) initial images of the sample at 0 s c) phase transition taking place at 50 s d) maximum temperature exposure at 75 s, e) and f) gradual cooling and g) back to room temperature.

Qiang Zhu: Conceptualization, Supervision, Funding acquisition

Declaration of competing interest

The authors declare that they have no known competing financial interests or personal relationships that could have appeared to influence the work reported in this paper.

Data availability

No data was used for the research described in the article.

Acknowledgement

This work was supported under the Structural Metal Alloy Program (SMAP), grant No. A18b1B0061, in Agency for Science, Technology and Research in Singapore.

References

[1] S. Jung, I. Ro, Strategic use of thermo-chemical processes for plastic waste valorization, Korean J. Chem. Eng. (2023) 1–13.
[2] D. Dussaux, S. Agrawala, Quantifying Environmentally Relevant and Circular Plastic Innovation: Historical Trends, Current Landscape and the Role of Policy, 2022.
[3] C. Wayman, H. Niemann, The fate of plastic in the ocean environment–a minireview, Environ. Sci.: Processes Impacts 23 (2) (2021) 198–212.
[4] J.K. Muiruri, J.C.C. Yeo, Q. Zhu, E. Ye, X.J. Loh, Z. Li, Poly (hydroxyalkanoates): production, applications and end-of-life strategies–life cycle assessment nexus, ACS Sustain. Chem. Eng. 10 (11) (2022) 3387–3406.
[5] H. Ballerstedt, T. Tiso, N. Wierckx, R. Wei, L. Averous, U. Bornscheuer, K. O'Connor, T. Floehr, A. Jupke, J. Klankermayer, MIXed plastics biodegradation and UPcycling using microbial communities: EU Horizon 2020 project MIX-UP started January 2020, Environ. Sci. Eur. 33 (1) (2021) 99.
[6] P.J. Ong, Z.X.J. Heng, Z. Xing, H.Y.Y. Ko, P. Wang, H. Liu, R. Ji, X. Wang, B.H. Tan, Z. Li, Wax from pyrolysis of waste plastics as a potential source of phase change material for thermal energy storage, Trans. Tianjin Univ. (2022) 1–10.
[7] J.K. Muiruri, J.C.C. Yeo, X.Y.D. Soo, S. Wang, H. Liu, J. Kong, J. Cao, B.H. Tan, A. Suwardi, Z. Li, Recent advances of sustainable short-chain length polyhydroxyalkanoates (Scl-PHAs)–plant biomass composites, Eur. Polym. J. 111882 (2023).
[8] X. Chen, Y. Wang, L. Zhang, Recent progress in the chemical upcycling of plastic wastes, ChemSusChem 14 (19) (2021) 4137–4151.
[9] M. Han, S. Zhu, C. Xia, B. Yang, Photocatalytic upcycling of poly (ethylene terephthalate) plastic to high-value chemicals, Appl. Catal. Environ. 316 (2022) 121662.
[10] S. Wang, J.K. Muiruri, X.Y.D. Soo, S. Liu, W. Thitsartarn, B.H. Tan, A. Suwardi, Z. Li, Q. Zhu, X.J. Loh, Bio-polypropylene and polypropylene-based biocomposites: solutions for a sustainable future, Chem. Asian J. 18 (2) (2023), e202200972.
[11] J. Zheng, S.F.D. Solco, C.J.E. Wong, S.A. Sia, X.Y. Tan, J. Cao, J.C.C. Yeo, W. Yan, Q. Zhu, Q. Yan, Integrating recyclable polymers into thermoelectric devices for green electronics, J. Mater. Chem. A 10 (37) (2022) 19787–19796.
[12] C. Lundell, J. Thomas, PET: polyethylene terephthalate–the ubiquitous 500 Ml water bottle, in: Advances in Industrial Design: Proceedings of the AHFE 2020 Virtual Conferences on Design for Inclusion, Affective and Pleasurable Design, Interdisciplinary Practice in Industrial Design, Kansei Engineering, and Human Factors for Apparel and Textile Engineering, July 16–20, 2020, Springer, USA, 2020, pp. 248–254.
[13] A. Turner, M. Filella, Field-portable-XRF reveals the ubiquity of antimony in plastic consumer products, Sci. Total Environ. 584 (2017) 982–989.
[14] P.J. Ong, Y. Leow, X.Y.D. Soo, M.H. Chua, X. Ni, A. Suwardi, C.K.I. Tan, R. Zheng, F. Wei, J. Xu, Valorization of spent coffee grounds: a sustainable resource for bio-based phase change materials for thermal energy storage, Waste Manag. 157 (2023) 339–347.
[15] Y.-H.V. Soong, M.J. Sobkowicz, D. Xie, Recent advances in biological recycling of polyethylene terephthalate (PET) plastic wastes, Bioengineering 9 (3) (2022) 98.
[16] R.v. Willige, J. Linssen, M. Meinders, H.v.d. Stege, A. Voragen, Influence of flavour absorption on oxygen permeation through LDPE, PP, PC and PET plastics food packaging, Food Addit. Contam. 19 (3) (2002) 303–313.
[17] P. Benyathiar, P. Kumar, G. Carpenter, J. Brace, D.K. Mishra, Polyethylene terephthalate (PET) bottle-to-bottle recycling for the beverage industry: a review, Polymers 14 (12) (2022) 2366.
[18] M. Khashij, M. Mokhtari, A. Dalvand, F. Haghiralsadat, H. Fallahzadeh, M. H. Salmani, Recycled PET/metal oxides nanocomposite membrane for treatment of real industrial effluents: membrane fabrication, stability, antifouling behavior, and process modeling and optimization, J. Mol. Liq. 364 (2022) 119966.
[19] C.-X. Shuai, Y. He, P. Su, Q. Huang, D. Pan, Q. Xu, D. Feng, Y. Jiang, Integration of PEGylated polyaniline nanocoatings with multiple plastic substrates generates comparable antifouling performance, Langmuir 36 (31) (2020) 9114–9123.
[20] J. Vartiainen, E. Skytta, J. Enqvist, R. Ahvenainen, Properties of antimicrobial plastics containing traditional food preservatives, Packaging Technol. Sci. Int. J. 16 (6) (2003) 223–229.
[21] X. Fan, B.H. Tan, Z. Li, X.J. Loh, Control of PLA stereoisomers-based polyurethane elastomers as highly efficient shape memory materials, ACS Sustain. Chem. Eng. 5 (1) (2017) 1217–1227.
[22] J.J.C. Lee, S. Sugiarto, P.J. Ong, X.Y.D. Soo, X. Ni, P. Luo, Y.Y.K. Hnin, J.S.Y. See, F. Wei, R. Zheng, Lignin-g-polycaprolactone as a form-stable phase change material for thermal energy storage application, J. Energy Storage 56 (2022) 106118.
[23] X.Y.D. Soo, Z.M. Png, M.H. Chua, J.C.C. Yeo, P.J. Ong, S. Wang, X. Wang, A. Suwardi, J. Cao, Y. Chen, A highly flexible form-stable silicone-octadecane PCM composite for heat harvesting, Mater. Today Adv. 14 (2022) 100227.
[24] X.Y.D. Soo, Z.M. Png, X. Wang, M.H. Chua, P.J. Ong, S. Wang, Z. Li, D. Chi, J. Xu, X.J. Loh, Rapid UV-curable form-stable polyethylene-glycol-based phase change material, ACS Appl. Polym. Mater. 4 (4) (2022) 2747–2756.
[25] X.Y. Soo, J.K. Muiruri, J.C. Yeo, Z.M. Png, A. Sng, H. Xie, R. Ji, S. Wang, H. Liu, J. Xu, Polyethylene glycol/polylactic acid block co-polymers as solid–solid phase change materials, SmartMat 4 (2023), e1188.
[26] H. Li, H. Chen, X. Li, J.G. Sanjayan, Development of thermal energy storage composites and prevention of PCM leakage, Appl. Energy 135 (2014) 225–233.
[27] J.J.C. Lee, N.J.X. Lim, P. Wang, H. Liu, S. Wang, C.-L.K. Lee, D. Kai, F. Wei, R. Ji, B. H. Tan, Silicon-containing additives in encapsulation of phase change materials for thermal energy storage, World Sci. Ann. Rev. Funct. Mater. 2230007 (2022).
[28] S. Ramakrishnan, J. Sanjayan, X. Wang, M. Alam, J. Wilson, A novel paraffin/expanded perlite composite phase change material for prevention of PCM leakage in cementitious composites, Appl. Energy 157 (2015) 85–94.
[29] H. Li, Z. Li, N. Li, X. Zhu, Y.F. Zhang, L. Sun, R. Wang, J. Zhang, Z. Yang, H. Yi, 3D printed high performance silver mesh for transparent glass heaters through liquid sacrificial substrate electric-field-driven jet, Small 18 (17) (2022) 2107811.
[30] X. Pan, W. Wu, X. Yu, L. Lu, C. Guo, Y. Zhao, Typical electrical, mechanical, electromechanical characteristics of copper-encapsulated REBCO tapes after processing in temperature under 250 °C, Supercond. Sci. Technol. 36 (3) (2023), 034004.
[31] L. Peng, Y. Sun, X. Gu, P. Liu, L. Bian, B. Wei, Thermal conductivity enhancement utilizing the synergistic effect of carbon nanocoating and graphene addition in palmitic acid/halloysite FSPCM, Appl. Clay Sci. 206 (2021) 106068.
[32] C. Chen, W. Liu, Z. Wang, K. Peng, W. Pan, Q. Xie, Novel form stable phase change materials based on the composites of polyethylene glycol/polymeric solid-solid phase change material, Sol. Energy Mater. Sol. Cells 134 (2015) 80–88.
[33] A. Wang, Y. Dou, X. Yang, Q. Wang, M.S. Sudi, L. Zhao, D. Shang, W. Zhu, J. Ren, Efficient oxygen evolution reaction from iron-molybdenum nitride/molybdenum oxide heterostructured composites, Dalton Trans. 52 (32) (2023) 11234–11242.
[34] H. Li, S. Zhao, W. Zhang, H. Du, X. Yang, Y. Peng, D. Han, B. Wang, Z. Li, Efficient esterification over hierarchical Zr-Beta zeolite synthesized via liquid-state ion-exchange strategy, Fuel 342 (2023) 127786.
[35] W. Zhao, H. Suo, S. Wang, L. Ma, L. Wang, Q. Wang, Z. Zhang, Mg gas infiltration for the fabrication of MgB2 pellets using nanosized and microsized B powders, J. Eur. Ceram. Soc. 42 (15) (2022) 7036–7048.
[36] C. Zhao, M. Xi, J. Huo, C. He, L. Fu, Computational design of BC3N2 based single atom catalyst for dramatic activation of inert CO2 and CH4 gasses into CH3COOH with ultralow CH4 dissociation barrier, Chin. Chem. Lett. 34 (1) (2023) 107213.
[37] C. Jia, X. Geng, F. Liu, Y. Gao, Thermal behavior improvement of hollow sintered bricks integrated with both thermal insulation material (TIM) and Phase-Change Material (PCM), Case Stud. Therm. Eng. 25 (2021) 100938.
[38] J. Cheon, S.-Y. Park, B.Y. Jeong, J.H. Chun, Preparation and properties of UV-curable polyurethane-acrylate coatings of pre-coated metal (PCM): effect of polyol type/contents on adhesive property, Mol. Cryst. Liq. Cryst. 706 (1) (2020) 62–71.
[39] X.J. Loh, Poly (DMAEMA-co-PPGMA): dual-responsive "reversible" micelles, J. Appl. Polym. Sci. 127 (2) (2013) 992–1000.
[40] A.K. Sani, I.O. Olawoore, R.M. Singh, Assessment of impregnating phase change materials into lightweight aggregates for development of thermal energy storage aggregate composites, Construct. Build Mater. 305 (2021) 124683.
[41] X.J. Loh, V.P.N. Nguyen, N. Kuo, J. Li, Encapsulation of basic fibroblast growth factor in thermogelling copolymers preserves its bioactivity, J. Mater. Chem. 21 (7) (2011) 2246–2254.
[42] L. Gan, G.R. Deen, X. Loh, Y. Gan, New stimuli-responsive copolymers of N-acryloyl-N′-alkyl piperazine and methyl methacrylate and their hydrogels, Polymer 42 (1) (2001) 65–69.
[43] W. Sun, Y. Liu, M. Li, Q. Cheng, L. Zhao, Study on heat flow transfer characteristics and main influencing factors of waxy crude oil tank during storage heating process under dynamic thermal conditions, Energy 269 (2023) 127001.
[44] J. Wang, Z. Pan, Y. Wang, L. Wang, L. Su, D. Cuiuri, Y. Zhao, H. Li, Evolution of crystallographic orientation, precipitation, phase transformation and mechanical properties realized by enhancing deposition current for dual-wire arc additive manufactured Ni-rich NiTi alloy, Addit. Manuf. 34 (2020) 101240.
[45] P. Xu, Q. Yuan, W. Ji, R. Yu, F. Wang, N. Huo, Study on the annealing phase transformation mechanism and electrochemical properties of carbon submicron fibers loaded with cobalt, Mater. Express 12 (12) (2022) 1493–1501.
[46] W. Xia, X. Fei, Q. Wang, Y. Lu, M.T. Innocent, J. Zhou, S. Yu, H. Xiang, M. Zhu, Nano-hybridized form-stable ester@ F-SiO2 phase change materials for melt-spun PA6 fibers engineered towards smart thermal management fabrics, Chem. Eng. J. 403 (2021) 126369.
[47] M.K. Ram, P.D. Myers Jr., C. Jotshi, D.Y. Goswami, E.K. Stefanakos, K.D. Arvanitis, E. Papanicolaou, V. Belessiotis, Microencapsulated dimethyl terephthalate phase change material for heat transfer fluid performance enhancement, Int. J. Energy Res. 41 (2) (2017) 252–262.

[48] N.A. Rorrer, S. Nicholson, A. Carpenter, M.J. Biddy, N.J. Grundl, G.T. Beckham, Combining reclaimed PET with bio-based monomers enables plastics upcycling, Joule 3 (4) (2019) 1006–1027.
[49] K. Fukushima, O. Coulembier, J.M. Lecuyer, H.A. Almegren, A.M. Alabdulrahman, F.D. Alsewailem, M.A. Mcneil, P. Dubois, R.M. Waymouth, H.W. Horn, Organocatalytic depolymerization of poly (ethylene terephthalate), J. Polym. Sci. A Polym. Chem. 49 (5) (2011) 1273–1281.
[50] R. Agrawal, J. Hanna, I.E. Gunduz, C.C. Luhrs, Epoxy–PCM composites with nanocarbons or multidimensional boron nitride as heat flow enhancers, Molecules 24 (10) (2019) 1883.
[51] S. Lashgari, A.R. Mahdavian, H. Arabi, V. Ambrogi, V. Marturano, Preparation of acrylic PCM microcapsules with dual responsivity to temperature and magnetic field changes, Eur. Polym. J. 101 (2018) 18–28.
[52] C. Amaral, S.C. Pinto, T. Silva, F. Mohseni, J.S. Amaral, V.S. Amaral, P.A.A. P. Marques, A. Barros-Timmons, R. Vicente, Development of polyurethane foam incorporating phase change material for thermal energy storage, J. Energy Storage 28 (2020) 101177.
[53] W.Y. Wu, G.M.D. Yeo, S. Wang, Z. Liu, X.J. Loh, Q. Zhu, Recent progress in polyethylene-enhanced organic phase change composite materials for energy management, Chem. Asian J. 18 (14) (2023), e202300391.
[54] Z. Chen, J.F. Wu, S. Fernando, K. Jagodzinski, Soy-based, high biorenewable content UV curable coatings, Prog. Org. Coat. 71 (1) (2011) 98–109.
[55] Z.M. Png, X.Y.D. Soo, M.H. Chua, P.J. Ong, J. Xu, Q. Zhu, Triazine derivatives as organic phase change materials with inherently low flammability, J. Mater. Chem. A 10 (7) (2022) 3633–3641.
[56] K. Nollenberger, J. Albers, Poly (meth) acrylate-based coatings, Int. J. Pharm. 457 (2) (2013) 461–469.
[57] C. Li, Q. Li, R. Ge, X. Lu, A novel one-step ultraviolet curing fabrication of myristic acid-resin shape-stabilized composite phase change material for low temperature thermal energy storage, Chem. Eng. J. 458 (2023) 141355.
[58] C. Decker, F. Masson, R. Schwalm, Weathering resistance of waterbased UV-cured polyurethane-acrylate coatings, Polym. Degrad. Stab. 83 (2) (2004) 309–320.
[59] Y. Feng, J. Hu, F. Wang, Q. Huang, C. Peng, Z. Xu, Synthesizing promising epoxy acrylate prepolymers applied in ultraviolet cured adhesives based on esterification reaction, Mater. Res. Express 5 (6) (2018), 065321.
[60] E. Yildirim, Q. Zhu, G. Wu, T.L. Tan, J. Xu, S.-W. Yang, Self-organization of PEDOT: PSS induced by green and water-soluble organic molecules, J. Phys. Chem. C 123 (15) (2019) 9745–9755.
[61] X. Miao, W. Zhu, Z. Zhang, W. Zhang, X. Zhu, J. Zhu, Photo-induced cobalt-mediated radical polymerization of vinyl acetate, Polym. Chem. 5 (2) (2014) 551–557.
[62] X.Y.D. Soo, Z.M. Png, X. Wang, M.H. Chua, P.J. Ong, S. Wang, Z. Li, D. Chi, J. Xu, X.J. Loh, Q. Zhu, Rapid UV-curable form-stable polyethylene-glycol-based phase change material, ACS Appl. Polym. Mater. 4 (4) (2022) 2747–2756.
[63] A. Sarı, G. Hekimog˘lu, Y. Karabayır, R.K. Sharma, H. Arslanog˘lu, O. Gencel, V. V. Tyagi, Capric-stearic acid mixture impregnated carbonized waste sugar beet pulp as leak-resistive composite phase change material with effective thermal conductivity and thermal energy storage performance, Energy 247 (2022) 123501.
[64] H. Alkhodairi, S.T. Russell, J. Pribyl, B.C. Benicewicz, S.K. Kumar, Compatibilizing immiscible polymer blends with sparsely grafted nanoparticles, Macromolecules 53 (23) (2020) 10330–10338.
[65] V.P.N. Nguyen, N. Kuo, X.J. Loh, New biocompatible thermogelling copolymers containing ethylene-butylene segments exhibiting very low gelation concentrations, Soft Matter 7 (5) (2011) 2150–2159.
[66] T. Tang, A.K.K. Kyaw, Q. Zhu, J. Xu, Water-dispersible conducting polyazulene and its application in thermoelectrics, Chem. Commun. 56 (65) (2020) 9388–9391.
[67] Q. Zhu, E. Yildirim, X. Wang, A.K.K. Kyaw, T. Tang, X.Y.D. Soo, Z.M. Wong, G. Wu, S.-W. Yang, J. Xu, Effect of substituents in sulfoxides on the enhancement of thermoelectric properties of PEDOT: PSS: experimental and modelling evidence, Mol. Syst. Des. Eng. 5 (5) (2020) 976–984.